ACS Macro Letters

Letter

pubs.acs.org/macroletters

# Optically Active Porous Materials Constructed by Chirally Helical Substituted Polyacetylene through a High Internal Phase Emulsion Approach and the Application in Enantioselective Crystallization

Junya Liang, Yi Wu, Xuesheng Deng, and Jianping Deng*

State Key Laboratory of Chemical Resource Engineering and College of Materials Science and Engineering, Beijing University of Chemical Technology, Beijing 100029, China

Supporting Information

**ABSTRACT:** This article reports the first optically active macroporous materials constructed by helical substituted polyacetylene and prepared by a high internal phase emulsion (HIPE) technique. The macroporous (~3 μm) materials were fabricated simply through polymerization of the continuous phase in HIPEs. The porous structures of the resulting materials can be adjusted by varying the fraction of the dispersed phase. The obtained materials were characterized by regular pore morphology, high porosity, and low density. Circular dichroism and UV−vis absorption spectra demonstrated that the substituted polyacetylene forming the materials adopted chirally helical conformations, which endowed the materials with considerable optical activity. The optically active porous materials were used as chiral inducers and efficiently induced enantioselective crystallization of threonine and alanine racemates. L-Threonine and L-alanine were preferably induced to form crystals from the respective racemic solutions. The prepared materials open a new type of functional chiral materials with potential applications in asymmetric catalysis, chiral resolution, etc.


Chiral porous materials have recently constituted an active research area in materials science.[1] They combine two important concepts, "chirality" and "porosity", in one entity. This distinctive feature renders the materials with intriguing properties, e.g., optical activity, low density, and high specific surface area. They have found significant applications in asymmetric catalysis,[2] enantioselective release,[3] chiral resolution,[4] etc. Unfortunately, chiral porous materials reported to date were primarily limited to inorganics (silica[5] and metals[6]) and organic−inorganic hybrids.[7] For chiral porous architectures solely constructed by organic polymers (chiral POPs), there have been only a few reports in the literature.[8−12] In particular notably, the chirality of such chiral POPs exclusively originated from configurational chirality (chiral small molecular units). Therefore, it still remains as a big challenge to construct chiral POPs by using synthetic helical polymers, in which the chirality is primarily contributed by conformational chirality (chiral helical structures).

In the present study, we prepared chiral POPs consisting of optically active helical substituted polyacetylenes through a straightforward technique, i.e., the high internal phase emulsion (HIPE) polymerization approach.[13,14] A variety of achiral advanced materials have been fabricated through HIPE and exhibited potential applications such as biomaterials[15] and separation materials.[16] Chiral helical substituted polyacetylenes are remarkably attractive as typical synthetic helical polymers[17−19] that show interesting chiral amplification effects.[20−23] Nowadays new synthetic helical polymers have been continuously established.[24−27] Our group has constructed chiral porous (or hollow) nano- and microscaled particles by helical substituted polyacetylenes.[8,28−30] On the basis of the previous studies, we further envision that the HIPE approach may be applicable for acetylenic monomers for preparing a novel, unique type of chiral porous materials. This contribution reports our exciting success—we not only established a versatile methodology for performing HIPE polymerizations of acetylentics (Figure 1), by which to have prepared the first chiral porous materials consisting of helical polymers, but also demonstrated their significant applications as chiral inducers for performing enantioselective crystallization.[31]

Three monomers (M1, M2, and M3) were synthesized as stated in the Supporting Information (SI, the same below) and used to prepare HIPEs. Two polymerization processes were involved (Figure 1A): coordination polymerization (A1) and radical polymerization (A2); the detailed processes are presented in the SI. A1 started from acetylenic monomer (M1 or M3) and proceeded through coordination polymerization. A2 started from a preformed helical macromonomer (M2) which underwent free radical (co)polymerization with/without butyl acrylate (BA). After polymerization and removing

Received: August 28, 2015
Accepted: October 5, 2015
Published: October 8, 2015





DOI: 10.1021/acsmacrolett.5b00613
ACS Macro Lett. 2015, 4, 1179−1183

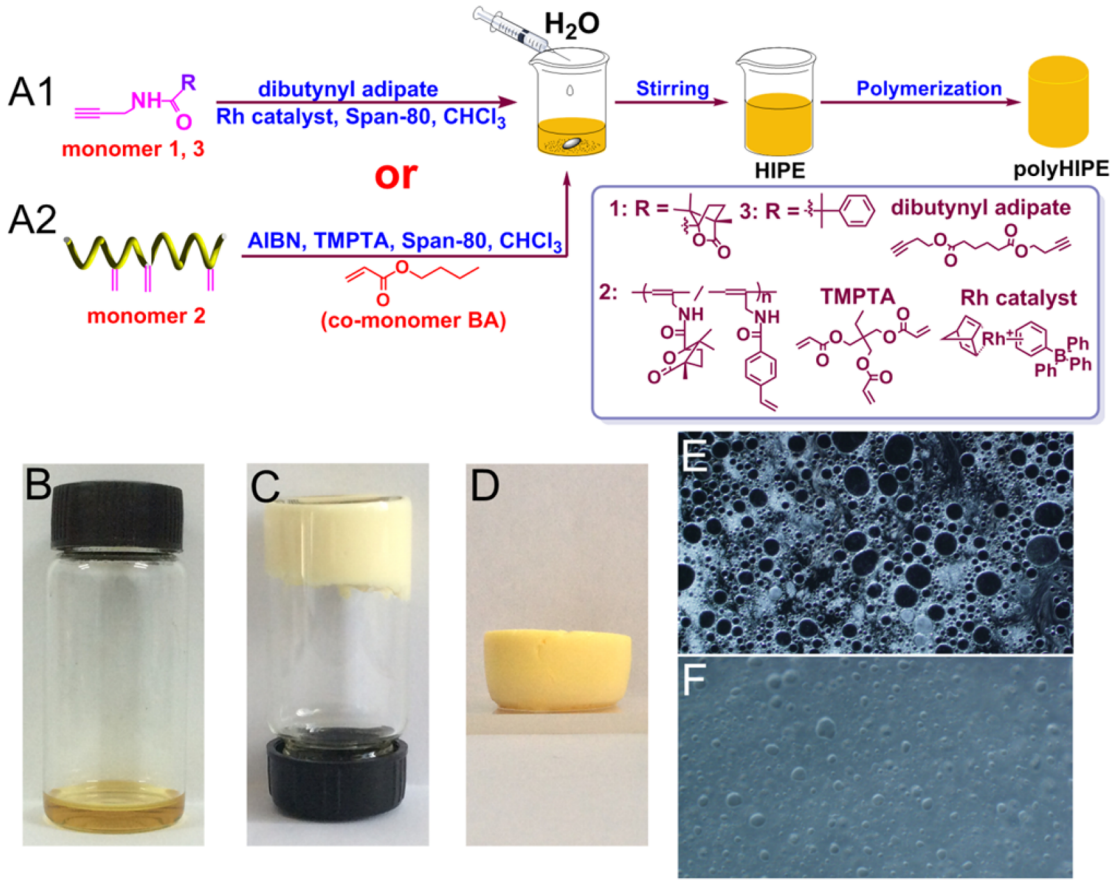


**Figure 1.** (A) Schematic for preparing polyHIPEs; typical photos of (B) continuous phase solution, (C) HIPE-2, (D) polyHIPE-2; optical microscopic images of (E) stable and (F) unstable HIPE.

the internal-phase water, HIPEs transferred into the corresponding polyHIPEs. We totally prepared seven HIPE samples, denoted as HIPE-1−7, for which the relevant information is listed in Table 1. PolyHIPE-1−3 were prepared by coordination polymerization with different water content (other conditions remained constant) to study the relationship between pore structure and water content. For polyHIPE-4 and 5, we prepared in advance the helical substituted polyacetylene bearing C═C pendent groups (M2) and used it as chiral macromonomer. M2 underwent radical polymerization (providing polyHIPE-4) and copolymerization with BA for providing polyHIPE-5. The purpose for preparing polyHIPE-4 and 5 is to provide an alternative route for preparing polyHIPEs consisting of helical polyacetylene. For polyHIPE-6 and 7, we intended to examine other substituted acetylenics as monomers, aiming at elucidating the wide applicability of the HIPE technique.

**Table 1. Formula for Preparing PolyHIPE-1−7**[a]

| | oil phase | | | water phase |
|---|---|---|---|---|
| sample | monomer | cross-linking agent | catalyst (initiator) | water content |
| polyHIPE-1 | M1 | dibutynyl adipate | Rh catalyst | 75% |
| polyHIPE-2 | M1 | dibutynyl adipate | Rh catalyst | 80% |
| polyHIPE-3 | M1 | dibutynyl adipate | Rh catalyst | 85% |
| polyHIPE-4 | M2 | TMPTA | AIBN | 80% |
| polyHIPE-5 | M2, BA | TMPTA | AIBN | 80% |
| polyHIPE-6 | M3 | dibutynyl adipate | Rh catalyst | 80% |
| polyHIPE-7 | –[b] | dibutynyl adipate | Rh catalyst | 80% |

[a]Span-80 and $CHCl_3$ were used as stabilizer and solvent, respectively. [b]Only cross-linking agent (dibutynyl adipate) was used.

All the above polyHIPE-1−7 were satisfactorily obtained. To prepare porous materials through the HIPE approach, it is important to ensure a stable HIPE, by which to avoid the transformation from homogeneous water-in-oil emulsion to two separated phases. As shown in Figure 1B, water was dropwise added in the oily continuous phase containing monomer, cross-linking agent, catalyst, and stabilizer under vigorous stirring. With an increase in water content, the emulsion system gradually lost its flowability and even became wholly frozen (Figure 1C). Thereby a homogeneous emulsion (HIPE) was formed and maintained the morphology for 2 weeks and above. In Figure 1C the HIPE was still fixed at the bottom of the vial though put upside down, clearly indicating the high stability of the HIPE. Figure 1D presents the corresponding polyHIPE after polymerization. For a vivid comparison, Figure 1 also illustrates the optical microscopic images of stable (Figure 1E) and unstable (Figure 1F) HIPEs.

The obtained polyHIPEs were observed by SEM, as shown in Figure 2. After removing the internal-phase water, the original droplets of dispersed phase left spherical pores inside the polyHIPEs. PolyHIPE-1−3 were, respectively, fabricated with 75, 80, and 85 vol % water content. They demonstrated



DOI: 10.1021/acsmacrolett.5b00613
ACS Macro Lett. 2015, 4, 1179−1183

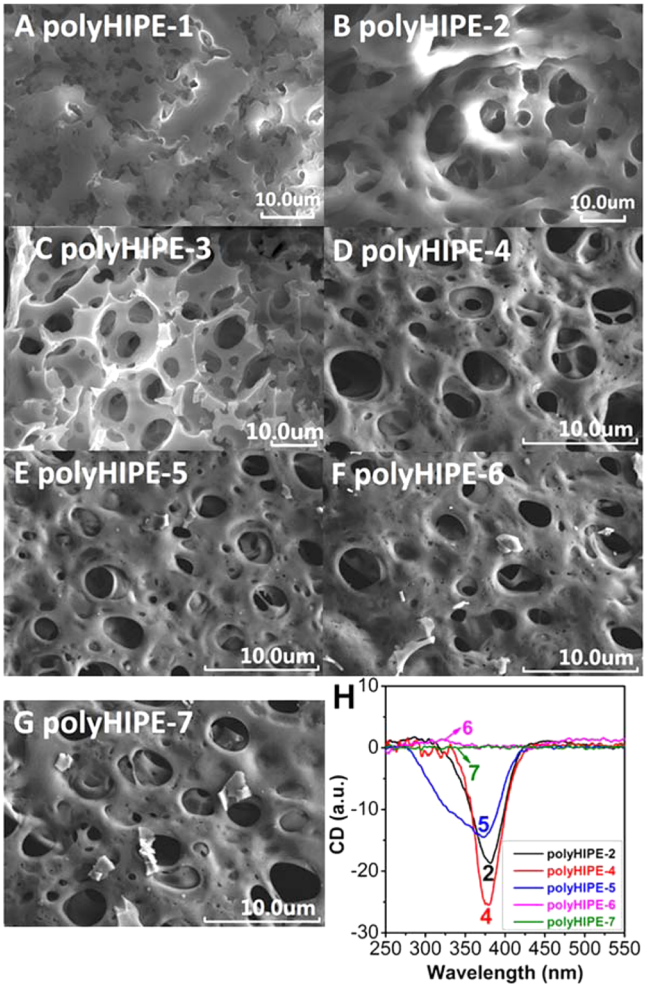


**Figure 2.** (A∼G) SEM images of polyHIPE-1−7 and (H) CD spectra of polyHIPE-2 and polyHIPE-4−7 measured by using pressed samples at room temperature.

that an increase in water content led to correspondingly increased pore size, specific surface area, and porosity (Figure 2A∼C, Table 2, and Figure S1), but the stability of the HIPEs still kept well. The apparent densities of polyHIPE-1−3 were much lower (approximately 0.1 g/cm$^3$) than common polymer materials and decreased with increasing water content. For the other four samples (polyHIPE-4−7), porous structures were also efficiently formed (Figure 2D∼G), clearly demonstrating the wide applicability of the HIPE technique for producing porous material.

To further verify the successful fabrication of polyHIPEs, the products were characterized by FT-IR spectroscopy (Figure S2), and the detailed analyses are provided in the SI, confirming the occurrence of polymerization. To explore the helical structures and optical activity of the polyHIPEs, they were qualitatively characterized by CD and UV−vis absorption spectroscopy techniques. In our previous studies,[30,32] the polymers derived from monomers like M1 and macromonomer (M2) exhibited intensive CD signals and UV−vis absorption around 350 nm due to the substituted polyacetylene chains adopting helical conformations with a predominantly one-handed screw sense. The polymers thus exhibited remarkable optical activity. The homopolymer of M3 had a UV−vis absorption peak at about 390 nm but failed to show any CD signal (300−500 nm) due to the helical conformations with both left- and right-handed helicity in an identical amount, so this polymer did not possess optical activity.[33] The polyHIPEs were cross-linked and could not dissolve in any solvent, so we could not measure CD and UV−vis absorption spectra quantitatively. Alternatively, the polyHIPEs were qualitatively tested by using compressed samples, a technique developed by us earlier.[30] The obtained CD spectra are illustrated in Figure 2H, and the corresponding UV−vis spectra are presented in Figure S3.

PolyHIPE-2 (a representative for polyHIPE-1−3), 4, and 5 exhibited intense CD signals and UV−vis absorption peaks around 375 nm, while polyHIPE-6 and 7 did not show any CD effect at wavelength ranging from 250 to 550 nm. Figure S3 shows that all the products had UV−vis absorption at 300−500 nm. The differences between the absorption intensity and the shifts in maximum wavelength are considered resulting from the specific measuring method, i.e., by using pressed samples as aforementioned. According to our earlier studies dealing with helical polyacetylenes,[28−30,32,34] the CD effects (Figure 2H) and UV−vis absorptions (Figure S3) indicate that the polyacetylene chains in polyHIPE-1−7 adopted helical structures; however, only the substituted polyacetylenes in polyHIPE-1−5 formed helical structures with a preferred handedness, facilitating the polyHIPEs to possess optical activity. By measuring Raman spectra (Figure S4), the *cis* content of polyHIPE-2 and 4−7 is 82, 70, 73, 87, and 90%, respectively.[35] The high *cis* content is favorable for the polymer chains to form helical structures. TGA analyses (Figure S5) further show the remarkable thermostability of the as-obtained polyHIPEs.

On the basis of the optical activity mentioned above, the porous materials in hand are expected to exhibit promising applications in chiral resolution. Enantioselective crystallization as one major method for chiral resolution has always been an active research topic.[31] In this contribution L-threonine and L-alanine were successfully induced to crystallize from the respective racemic solution. Herein threonine racemate was taken for performing enantioselective crystallization by using the chiral porous polyHIPEs (polyHIPE-2) as chiral inducers. The porosity in polyHIPEs would increase the area of nucleation sites, thus increasing the crystallization rate. A detailed enantioselective crystallization procedure is described in the SI. We highlight that the pore structure in polyHIPEs has a positive effect on the full contact between racemates and polyHIPEs which is required for achieving high enantiomeric excess (ee) in the induced crystals; meanwhile, the bulk polyHIPEs were extremely easily recycled from the induced

**Table 2. Pore Analysis and Apparent Density of PolyHIPE-1−3**

| sample | water content (vol %) | mean pore diameter ($\mu$m) | specific pore volume (cm$^3$/g) | specific surface area (m$^2$/g) | porosity (%) | apparent density (g/cm$^3$) |
|---|---|---|---|---|---|---|
| polyHIPE-1 | 75 | 2.45 | 1.09 | 10.85 | 72.3 | 0.113 |
| polyHIPE-2 | 80 | 2.71 | 1.46 | 15.26 | 77.6 | 0.106 |
| polyHIPE-3 | 85 | 3.00 | 1.63 | 18.62 | 81.1 | 0.099 |



DOI: 10.1021/acsmacrolett.5b00613
*ACS Macro Lett.* 2015, 4, 1179−1183

crystals. SEM images of the induced threonine crystals are presented in Figure 3.

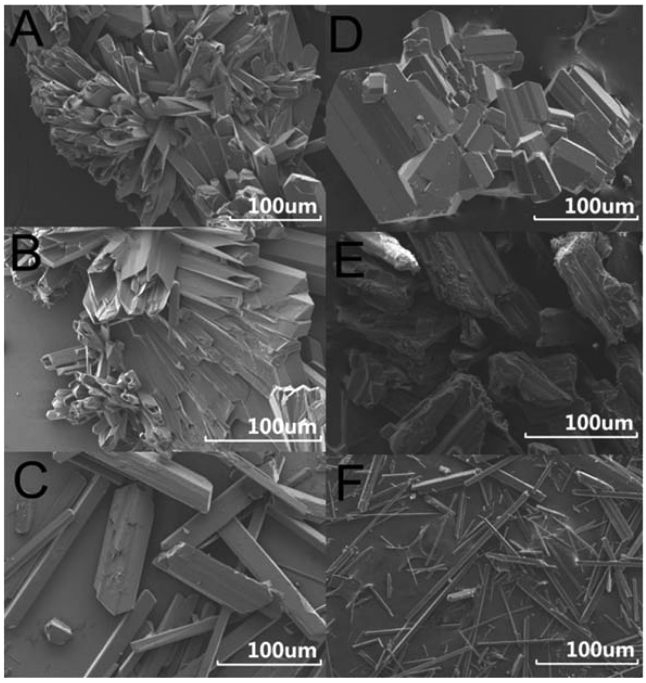


**Figure 3.** SEM images of threonine crystals induced through enantioselective crystallization: (A) without additive, (B) by polyHIPE-6, (C) by polyHIPE-2; and alanine crystals through enantioselective crystallization: (D) without additive, (E) by polyHIPE-6, (F) by polyHIPE-2.

As reference experiments, crystallization of racemic threonine was also performed without using any additive and with optically inactive polyHIPE-6 as additive. Both the crystallization processes were performed in the same way as in the case using polyHIPE-2. The SEM images presented in Figure 3A and 3B show that for the threonine crystals obtained without any additive and by using polyHIPE-6 as additive crystal clusters with tubular morphology were observed. These crystals were subsequently verified consisting of both D- and L-threonines in equal amounts (see below). For the threonine crystals induced by polyHIPE-2, clean and solid rectangular-like crystals were observed in Figure 3C. The crystals were subjected to X-ray diffraction (XRD) analysis (Figure S6). For a vivid comparison, we also conducted XRD analysis of pure L-threonine and racemic threonine. The patterns for pure L-threonine and the threonine crystals induced by polyHIPE-2 are considered being the same but noticeably different from racemic threonine crystals. So we preliminarily conclude that the rectangular-like crystals induced by polyHIPE-2 were primarily constructed by L-threonine. This conclusion is further supported by CD measurements, as shown in Figure S7A (the corresponding UV−vis spectra are shown in Figure S7B). As the concentration of the residual solution was indefinite, the CD and UV spectra were qualitatively measured. Like pure L-threonine, the L-threonine crystals induced by polyHIPE-2 exhibited a positive CD signal at an identical wavelength ($\lambda_{max}$ = 209 nm), whereas the residual solution showed a negative signal at the corresponding wavelength. Both the CD spectra of the threonine crystals obtained without any additive and induced by polyHIPE-6 showed no CD signals (Figure S7A). In the enantioselective crystallization induced by polyHIPE-2, the chiral separation efficiency was further investigated. The enantiomeric excess (ee) was 74%, and the crystal yield was 36%. The low crystal yield may be related to the types of the solvent, the amount of the solvent, the time of enantioselective crystallization, and the amount of chiral inducer.

The investigations presented above convincingly demonstrate the essential role of chiral polyHIPE-2 in inducing enantioselective crystallization of racemic threonine. Besides threonine, chiral polyHIPE-2 also successfully induced racemic alanine to undergo enantioselective crystallization. In this case L-alanine was preferentially induced to crystallize, and the relevant results are presented in Figure 3D∼F and Figures S8∼S9 (SI). The results further evidenced the potential applications of the novel chiral porous polyHIPEs. Apart from being used as chiral inducers for enantioselective crystallization, we are convinced that the polyHIPEs hold other significant potentials, e.g., as chiral reactors toward asymmetric catalysis. It is worthy to mention that we also tested the oil adsorption of the materials, which is a guarantee for reactants swelling into the pores to react. The results showed that the polyHIPEs had noticeable oil adsorption (33 g/g toward $CHCl_3$, max.) and reusability (the oil adsorption process could be repeated for at least 5 times only with slight loss in oil adsorption ability); the detailed data are shown in Figure S10, which provides evidence for the potential applications of polyHIPEs as chiral reactors.

In conclusion, we established an efficient strategy for performing HIPE polymerization of acetylenics and prepared unprecedented chiral porous materials based on helical substituted polyacetylene. The pore size, polydispersity of the pores, and the specific surface area of the porous materials can be easily adjusted by varying the fraction of the dispersed phase water. Enantioselective crystallization was efficiently induced by using the chiral porous polyHIPE. An ee over 70% was achieved in threonine. We anticipate that enantioselective crystallization can be realized for more racemic compounds. Also of significant importance is the successful establishment of HIPE methodology, by which a series of novel chiral and achiral porous materials can be prepared with acetylenic monomers. Apart from inducing enantioselective crystallization, other potential applications of the novel chiral polyHIPEs are currently under investigation. We expect that the pores inside the polyHIPEs may act as chiral reactors for performing asymmetric catalysis; the bulk chiral polyHIPEs can be used as monolithic columns for chiral separation. The fascinating materials and the significant potentials deserve much more exploration.

## ■ ASSOCIATED CONTENT

### Supporting Information

The Supporting Information is available free of charge on the ACS Publications website at DOI: 10.1021/acsmacrolett.5b00613.

Materials, experimental details, and supplementary data (PDF)

## ■ AUTHOR INFORMATION

### Corresponding Author

*E-mail: dengjp@mail.buct.edu.cn.

### Notes

The authors declare no competing financial interest.



DOI: 10.1021/acsmacrolett.5b00613
ACS Macro Lett. 2015, 4, 1179−1183

## ■ ACKNOWLEDGMENTS

This work was supported by the National Natural Science Foundation of China (21474007, 21274008, 21174010) and the Funds for Creative Research Groups of China (51221002).

## ■ REFERENCES

(1) Qiu, H.; Che, S. *Chem. Soc. Rev.* **2011**, *40*, 1259−1268.
(2) Zhang, Z.; Ji, Y. R.; Wojtas, L.; Gao, W.-Y.; Ma, S.; Zaworotko, M. J.; Antilla, J. C. *Chem. Commun.* **2013**, *49*, 7693−7695.
(3) Sun, C.-Y.; Qin, C.; Wang, C.-G.; Su, Z.-M.; Wang, S.; Wang, X.-L.; Yang, G.-S.; Shao, K.-Z.; Lan, Y.-Q.; Wang, E.-B. *Adv. Mater.* **2011**, *23*, 5629−5632.
(4) Spudeit, D. A.; Dolzan, M. D.; Breitbach, Z. S.; Barber, W. E.; Micke, G. A.; Armstrong, D. W. *J. Chromatogr. A* **2014**, *1363*, 89−95.
(5) Shopsowitz, K. E.; Qi, H.; Hamad, W. Y.; MacLachlan, M. J. *Nature* **2010**, *468*, 422−425.
(6) Wattanakit, C.; Saint Côme, Y. B.; Lapeyre, V.; Bopp, P. A.; Heim, M.; Yadnum, S.; Nokbin, S.; Warakulwit, C.; Limtrakul, J.; Kuhn, A. *Nat. Commun.* **2014**, *5*, 3325−3332.
(7) Wanderley, M. M.; Wang, C.; Wu, C.-D.; Lin, W. *J. Am. Chem. Soc.* **2012**, *134*, 9050−9053.
(8) Chen, C.; Zhao, B.; Deng, J. *ACS Macro Lett.* **2015**, *4*, 348−352.
(9) Ma, L.; Wanderley, M. M.; Lin, W. *ACS Catal.* **2011**, *1*, 691−697.
(10) Dong, J.; Liu, Y.; Cui, Y. *Chem. Commun.* **2014**, *50*, 14949−14952.
(11) An, W. K.; Han, M. Y.; Wang, C. A.; Yu, S. M.; Zhang, Y.; Bai, S.; Wang, W. *Chem. - Eur. J.* **2014**, *20*, 11019−11028.
(12) Paik, P.; Gedanken, A.; Mastai, Y. *J. Mater. Chem.* **2010**, *20*, 4085−4093.
(13) Schüler, F.; Schamel, D.; Salonen, A.; Drenckhan, W.; Gilchrist, M. D.; Stubenrauch, C. *Angew. Chem., Int. Ed.* **2012**, *51*, 2213−2217.
(14) Kimmins, S. D.; Cameron, N. R. *Adv. Funct. Mater.* **2011**, *21*, 211−225.
(15) Hayward, A. S.; Sano, N.; Przyborski, S. A.; Cameron, N. R. *Macromol. Rapid Commun.* **2013**, *34*, 1844−1849.
(16) Pulko, I.; Krajnc, P. *Macromol. Rapid Commun.* **2012**, *33*, 1731−1746.
(17) Yashima, E.; Maeda, K.; Iida, H.; Furusho, Y.; Nagai, K. *Chem. Rev.* **2009**, *109*, 6102−6211.
(18) Liu, J.; Lam, J. W. Y.; Tang, B. Z. *Chem. Rev.* **2009**, *109*, 5799−5867.
(19) Rudick, J. G.; Percec, V. *Acc. Chem. Res.* **2008**, *41*, 1641−1652.
(20) Jain, V.; Cheon, K.-S.; Tang, K.; Jha, S.; Green, M. M. *Isr. J. Chem.* **2011**, *51*, 1067−1074.
(21) Markvoort, A. J.; ten Eikelder, H. M. M.; Hilbers, P. A. J.; de Greef, T. F. A.; Meijer, E. W. *Nat. Commun.* **2011**, *2*, 509−517.
(22) Wulff, G.; Matussek, A.; Hanf, C.; Gladow, S.; Lehmann, C.; Goddard, R. *Angew. Chem., Int. Ed.* **2000**, *39*, 2275−2277.
(23) Wulff, G.; Gladow, S.; Krieger, S. *Macromolecules* **1995**, *28*, 7434−7440.
(24) Teraguchi, M.; Tanioka, D.; Kaneko, T.; Aoki, T. *ACS Macro Lett.* **2012**, *1*, 1258−1261.
(25) Yoshida, Y.; Mawatari, Y.; Motoshige, A.; Motoshige, R.; Hiraoki, T.; Wagner, M.; Müllen, K.; Tabata, M. *J. Am. Chem. Soc.* **2013**, *135*, 4110−4116.
(26) San Jose, B. A.; Yan, J.; Akagi, K. *Angew. Chem., Int. Ed.* **2014**, *53*, 10641−10644.
(27) Freire, F.; Seco, J. M.; Quiñoá, E.; Riguera, R. *J. Am. Chem. Soc.* **2012**, *134*, 19374−19383.
(28) Chen, B.; Deng, J.; Yang, W. *Adv. Funct. Mater.* **2011**, *21*, 2345−2350.
(29) Chen, B.; Deng, J.; Liu, X.; Yang, W. *Macromolecules* **2010**, *43*, 3177−3182.
(30) Liang, J.; Song, C.; Deng, J. *ACS Appl. Mater. Interfaces* **2014**, *6*, 19041−19049.
(31) Preiss, L. C.; Werber, L.; Fischer, V.; Hanif, S.; Landfester, K.; Mastai, Y.; Muñoz-Espí, R. *Adv. Mater.* **2015**, *27*, 2728−2732.
(32) Li, W.; Liu, X.; Qian, G.; Deng, J. *Chem. Mater.* **2014**, *26*, 1948−1956.
(33) Deng, J.; Tabei, J.; Shiotsuki, M.; Sanda, F.; Masuda, T. *Macromolecules* **2004**, *37*, 7156−7162.
(34) Luo, X.; Deng, J.; Yang, W. *Angew. Chem., Int. Ed.* **2011**, *50*, 4909−4912.
(35) Tabata, M.; Fukushima, T.; Sadahiro, Y. *Macromolecules* **2004**, *37*, 4342−4350.



DOI: 10.1021/acsmacrolett.5b00613
*ACS Macro Lett.* 2015, 4, 1179−1183